# Physics potential of timing layers for future detectors

S.V. Chekanov[a], A.V. Kotwal[c], C.-H. Yeh[b], S.-S. Yu[b]

[a] *HEP Division, Argonne National Laboratory, 9700 S. Cass Avenue, Argonne, IL 60439, USA.*
[b] *Department of Physics and Center for High Energy and High Field Physics, National Central University, Chung-Li, Taoyuan City 32001, Taiwan*
[c] *Department of Physics, Duke University, USA*

**Abstract**

The physics potential of timing layers with a few tens of pico-second resolution for calorimeters of future detectors used in particle-collision experiments is explored. The presented studies show how such layers can be used for identification of separate particles, as well as illustrate the benefit of using such detectors for detection of new event signatures beyond the Standard Model.

*Keywords:*

## 1. Introduction

Future experiments, such as CLIC [1], International Linear Collider (ILC) [2], high-energy LHC (HE-LHC), future circular *pp* colliders of the European initiative, FCC-hh [3] and the Chinese initiative, SppC [4] will require high precision measurements of particle and jets at large transverse momenta. The usage of timing information for such experiments can provide additional information that can be used to improve particle and jet reconstruction, as well as to reduce background events. For CLIC and FCC, high-precision time stamping of calorimeter energy deposits will be essential for background rejection (i.e. fake energy deposits) and pile-up mitigation. Precise timing information can be used to improve reconstruction of particle flow objects by reducing overlap of energy showers in high-granular calorimeters.

From the physics point of view, timing layers can be used for detection of long-lived particles and identification of Standard Model particles. At this moment, conceptional design reports for future experiments did not fully explore the benefits of the time of flight (TOF) measurements with tens-of-picosecond resolutions for calorimeters.

In this paper we will investigate the benefits of the timing layers with the resolution in the range 10 ps – 1 ns for Standard Model (SM) measurements of particles. The resolution of 1 ns is quite standard for the existing and planned calorimeters, and is only used as a benchmark for comparisons with more challenging 10 – 20 ps resolution devices. In addition, we investigate the capabilities of timing layers for identification of heavy stable particles which may be produced beyond the Standard Model (BSM).

*Email addresses:* chekanov@anl.gov (S.V. Chekanov), ashutosh.kotwal@duke.edu (A.V. Kotwal), a9510130375@gmail.com (C.-H. Yeh), syu@cern.ch (S.-S. Yu)

We hope such studies can help shape the requirements for future calorimeters, which were already outlined in the CPAD report [5] that emphasizes the need to develop fast timing for calorimeter measurements.

## 2. Proposal

A generic design of hadronic (electromagnetic) calorimeters for future particle collision experiments (HE-LHC, FCC, CLIC, ILC etc.) is based on two main characteristics: (1) high-granularity calorimeters with cells ranged from $3 \times 3$ mm$^2$ (for ECAL) to $5 \times 5$ cm$^2$ (for HCAL) in sizes. (2) timing with a nanosecond precision that improves background rejection, vertex association, and detection of new particles. According to the CPAD report [5], a development of "picosecond time resolution" for future calorimeters is one of the critical needs. Presently, high-granularity calorimeters (with ¿1 millions channels) with tens of picoseconds resolution represent a significant challenge due the large cost.

As a part of the HL-LHC upgrade program, CMS and ATLAS experiments are designing high-precision timing detectors with the time resolution of about 30 ps. They are based on silicon sensors that add an extra "dimension to event reconstruction. Such timing capabilities are not fully explored for future detectors beyond the HL-LHC upgrade. High-precision timing will be beneficial for new physics searches and b-tagging for all post-LHC experiments. For CLIC and FCC, high-precision time stamping will be essential for background rejection and pile-up mitigation.

Currently, the baseline designs of the high-granularity ECAL and HCAL of the CLIC/FCC detectors have not been optimized for precision timing in the range of a few tens of picoseconds. The latter is considered as an expensive option for many mullions of channels of these high-granularity detectors. This opens an opportunity to investigate a cost-effective "timing layer" (with the time resolution of smaller than 30 ps) for the post-LHC detectors. This layer will be installed on front of high-granularity calorimeters, covering both the forward and barrel regions.

In this paper we will investigate physics advantages of installing timing layers in the front of calorimeters of the post-LHC experiments. Typically, thin detectors on front of calorimeters are called "preshower", and they have been installed for the ZEUS, CDF and ATLAS experiments. The design goal of such detectors is to count the number of charged particles in order to correct for energy losses. The timing information of "mips" (minimumionising particles) is not used for particle identifications, nor precise timing. Unlike the standard pre-shower detector, we propose not only count mips, but also reconstruct high-precision timing and the position. This timing detector will have a similar granularity as the proposed high-granularity electromagnetic calorimeters themselves, but will have the sensor technology and the readout which are best suited for time stamping of mip signals (not necessarily for energy reconstruction). Our proposal is to enclose the EM detectors with two timing layers, one - before the first EM layer, and the second is after the last EM layer (but before the HCAL). The two layers of the timing detector allow a robust identification of time by correlating the position and timestamps of the particle passing through the ECAL.

In this paper we will explore this idea using semi-analytical approach and Monte Carlo simulations. A schematic representation of the positions of the timing layers for

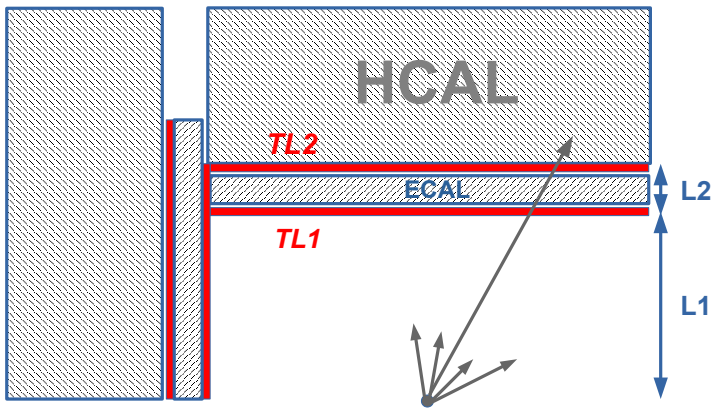


Figure 1: An example of positions of the thin timing layers for a generic detector. The thin timing layers will enclose the electromagnetic calorimeter, allow a reliable reconstruction of the mip signals with a timing resolution of the order of 10 ps.

a generic detector geometry is shown in Fig. 1 In the following, the first timing layer (closest to the interaction point) will be called TL1, while the second timing layer after the electromagnetic calorimeter will be called TL2.

There are several reasons why the second timing layer (TL2) can be useful:

- It can be used to measure the time of flight between TL2 and TL1 for identification of stable massive particles without known production vertex. This is especially important since the current detectors do not have acceptance for models where the production vertex of the stable heavy particles is close to the surface of the electromagnetic calorimeter.

  The distance between TL2 and TL1 is typically 0.2 – 0.4 m (depending on the design of the electromagnetic calorimeter), and it is not immediately obvious that such small distance can be used for physics measurements. A particle traveling with the speed of light can cross the distance between TL1 and TL1 within $\sim$ 1 ns. As we will discuss later, this distance is sufficient for heavy particle identification for 10 – 20 ps detectors.

- Two layers are useful in the cases when a long lived particle (neutral or charged) is produced without precise knowledge of the primary vertex (0,0,0) due to the beam (or pileup) smearing.

- It allows to correlate the hits with the first layer, and thus provides directionality of the hits. This feature can be useful to match the hits with the calorimeter cells

and to deal with back-scatter hits which are typically arriving from the hadronic calorimeter at later time.

- It provides the redundancy for TOF measurements.

The second layer of the timing detector can be justified if the recorded time difference for hits in the electromagnetic showers is not significantly different from that expected from a particle traveling with the speed of light. In order to verify this, we used a full Geant4 (version 10.3) [6] simulation of the SiFCC detector [7] that allows to use the information on hits from the ECAL. The ECAL is built from a highly segmented silicon-tungsten cells with the transverse size of $2 \times 2$ cm. The ECAL has 30 layers built from tungsten pads with silicon readout, corresponding to 35 $X_0$. The first 20 layers use tungsten of 3 mm thickness. The last ten layers use tungsten layers of twice the thickness, and thus have half the sampling fraction. The distance between the centers of the last and first ECAL layer is about 240 mm.

To verify that the time differences between last and first layer of ECAL is close to the time required for a particle that travels with the speed of light, and can be neglected for the timing layers that have a timing resolution of the order of 1 ns, a sample of single pions was created with 1 and 10 GeV momentum. The pseudorapidity for all such particles was $\eta = 0$ (central region). The particles were reconstructed in the ECAL calorimeter, and the time difference $\Delta T = T_{\text{last}} - T_{\text{first}}$ of the hits between the last and first ECAL layers was calculated. Only hits that arrive first were considered.

Figure 2 shows the time distribution for 1 and 10 GeV pions. It can be seen that the peak positions of the distributions are smaller than 1 ns, as expected for the distance of about 20 cm between the centers of the last and first layers. Therefore, hits will be simultaneous for the standard 1 ns resolution, i.e. well correlated in time and are identified as a single crossing particle. If a resolution of the timing layer will be of the order of 10 – 20 ps, a physics measurement of TOF would be possible.

Figure 2 also shows the hit distribution for (anti)deutrons, denoted as $d^{\pm}$. The distribution are significantly different from $\pi^{\pm}$. On average, 1 GeV (anti)deutrons should be measured with the time delay of 0.7 – 1.4 ns between the last and first layers. The value of 0.7 ns was estimated from the mean position of the Landau distribution used to fit the $d^{\pm}$ curve presented in Figure 2(a), while 1.4 ns was obtained for the mean of this distribution. Even for the most conservative 0.7 ns value, there is an indication that 1 GeV deutrons can be separated from pions that have 0.5 ns time difference. Such a separation can be observed when using a tens-of-picosecond detector. For 10 GeV particles presented in Figure 2(b), separation between $d^{\pm}$ and $\pi^{\pm}$ cannot be observed.

In summary, we have illustrated that a typical difference between TL2 and TL1 (which is approximated by the difference between the last and first layer of the electromagnetic calorimeter) is sufficient for particle identification using the TOF. As an example, a $d^{\pm}$ can be identified and separated from pions for the momentum less than 1 GeV. This means that heavier than deutron particles can also be identified for a momentum larger than 1 GeV. In the following, we will abstract from the full simulations and calculate the kinematic regions where identification of heavy stable particles is possible.

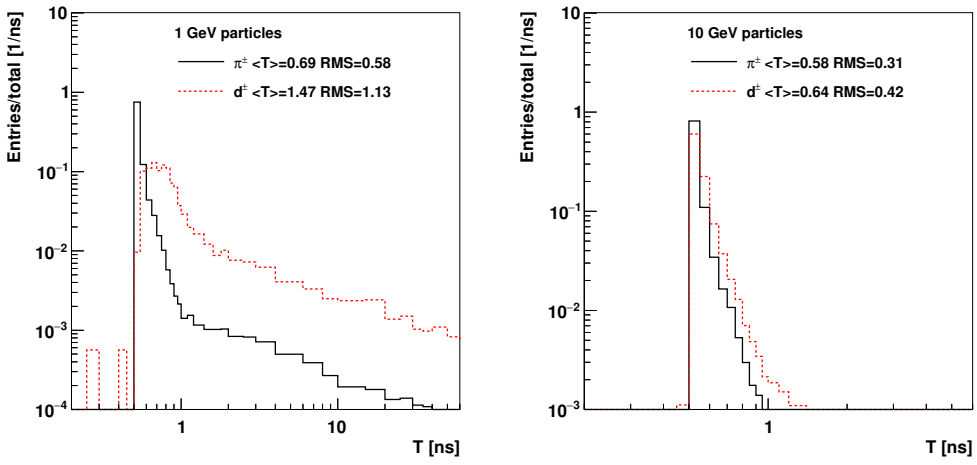


(a) (b)

Figure 2: The difference between time of hits between the last and first layer of ECAL for single pions and deutrons with the transverse momentum 1 and 10 GeV. Only first (fastest) hits were considered to calculate the difference in TOF.

## 3. Timing layers for single particles

Now let us discuss the kinematic regions for the TOF measurements in relation to either SM particles or BSM particles.

For an estimation of the separation power between different mass hypotheses, we will calculate the mass and momentum for which one can achieve separation significance higher than $3\sigma$ (or $p$-val$< 0.03$) If we have two particles with masses $m$ and a reference (fixed) mass $m_F$, the $3\sigma$ separation can be achieved assuming this condition [8]:

$$\frac{L}{c\sigma_{\rm TOF}}\left|\sqrt{1+\frac{m^2}{p^2}}-\sqrt{1+\frac{m_F^2}{p^2}}\right|>3 \tag{1}$$

where $p$ is the momenta of particles, $L$ is the length of the particle trajectory, and $\sigma_{TOF}$ is the resolution of the timing layer that measures the TOF.

Figure 3 shows the $3\sigma$ separation from the pion mass hypothesis ($m_F = m_\pi$) using the same procedure as discussed in [8]. The calculations are performed for several options for the resolution of the timing layer, from 10 ps to 1 ns, as a function of the travel length $L$ and the momenta. For a 20 ps detector and for a typical travel distance of $L \sim 0.2$ m from the interaction point to the electromagnetic calorimeter, neutrons (and protons) can be separated from the pion hypothesis up to 7 GeV. The separation of $K-$mesons can be performed up to 3 GeV. This momentum range should be sufficient for reliable particle identification in a wide range of physics studies, especially if such identification is used for jets that are dominated by this momentum range of separate particles. For a detector with 1 ns, the separation can only be possible up to 300 – 500 MeV. This is below than a typical minimum transverse momentum of 0.5 – 1 GeV for particles considered for high-energy proton colliders . Therefore, a timing layer with 1 ns resolution cannot effectively be used for particle identification in such experiments.

Having discussed a rather obvious case of identification of neutrons (or protons) and the $K$-mesons from the pion hypothesis, let us turn to the BSM searches for heavy particles. The most abundant SM background for light BSM particles from primary interactions are protons and neutrons. Other stable particles, that can be produced mainly in detector material (or from the interaction in the beam pipe) and detected by calorimeter are deutrons and $\alpha$ particles (composed from two protons and two neutrons). Although the rate of $\alpha$ particles sh be low since such particles can easy be stopped by detector material, it is not impossible that residual rate may still represent background for BSM searches that have a lower production rate. Therefore, we will choose $m_F = m_\alpha \simeq 3.73$ GeV for Eq. 1 and evaluate the $3\sigma$ separation for a wide range of masses and momentum. For most future experiments the distance between the interaction point and the first layer of the electromagnetic calorimeter is $L = 1.5 - 2.5$ m. For a representative purpose, we will use $L = 2$ m and consider 0.2 m for the separation distance between the TL2 and TL1 timing layers.

Figure 4 shows the particle identification power for different choices of the timing layer resolution and the distance $L = L_1$ to the first timing layer (see Fig. 1). For $L = L_1 = 2$ m, one can be see that a stable heavy particle with a mass of 100 GeV can be reconstructed up to 400 GeV assuming a 20 ns timing layer, but only up to 50 GeV using the standard 1 ns calorimeter.

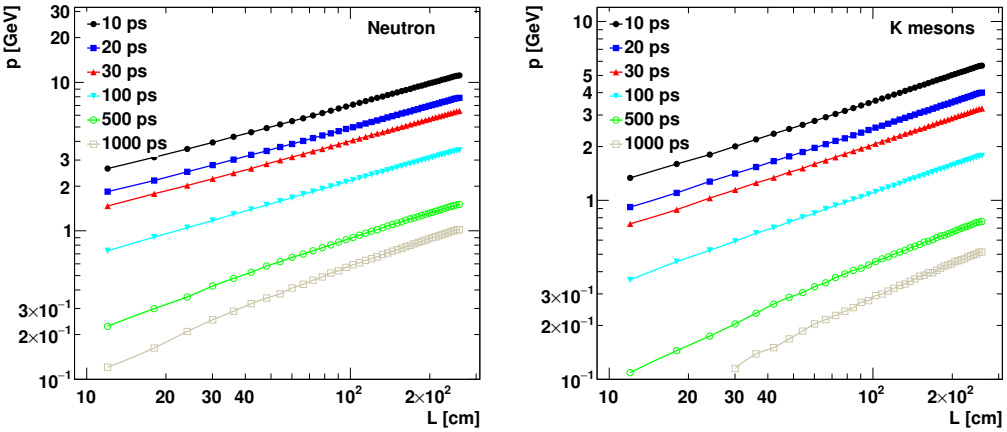


(a) Neutrons (b) $K$-mesons

Figure 3: The $3\sigma$ separation from the pion mass for neutrons and $K$-mesons as a function of the distance and the momenta.

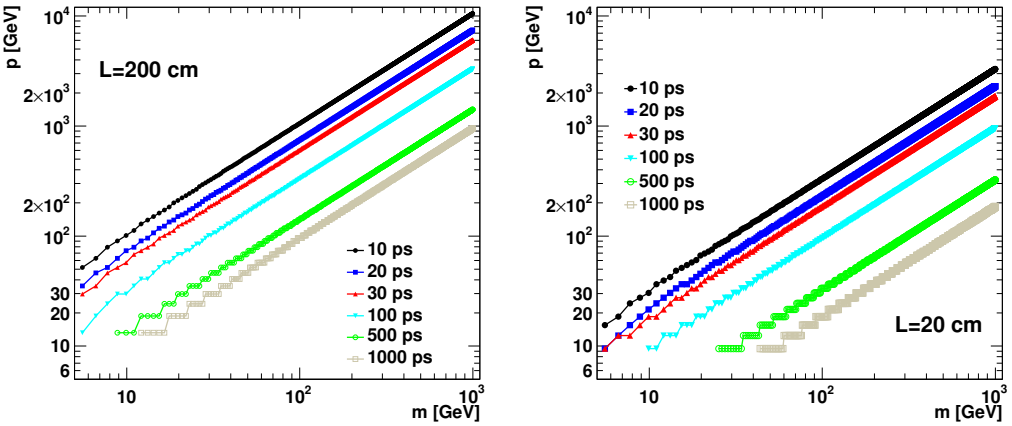


(a) for $L = 2$ m (b) for $L = 0.2$ m

Figure 4: The $3\sigma$ identification for heavy particles assuming timing layers with different resolutions for TOF, and using $L = 2$ m and $L = 0.2$ m. The first value is a typical distance from the vertex to the first layer ($TL_1$), while the second value is the typical distance between two timing layers enclosing an electromagnetic calorimeter, assuming a typical calorimeter based on the silicon technology.

One can also consider a measurement that does not involve a priory knowledge of the vertex, thus can be better designed for neutral particles in collisions with large pile-up (multiple number of vertexes). In the case the TOF is measured between the two layers, TL1 and TL2, assuming a successful spacial match of the hits.

The identification power in the case when the distance between TL2 and TL1 is 0.2 m is shown in Figure 4(b). For a 100 GeV stable particle, the identification is possible up to about 100 GeV. The standard calorimeter with 1 ns resolution can perform the identification up to 20 GeV.

## 4. Showcase for the Dark QCD model

The arguments discussed before can be illustrated using a concrete physics scenario. In particular, we will consider the dark QCD model [9, 10] which predicts "emerging" jets that are created in the decays of new long-lived neutral particles (dark hadrons), produced in a parton-shower process by dark QCD. The process include two mediators with masses $Mx$, each of which decays to a Standard Model quark and a dark quark. The final-state signature consists of four high transverse momentum jets, two of which are from two from dark quarks. These two "emerging" jets contain many displaced vertices arising from the decays of the dark pions produced in the dark parton shower.

Recently searches for such emerging jets have been performed [11] by the CMS Collaboration. The emerging jet contains multiple displaced vertices and thus multiple tracks with large pact parameters. Assuming that the mass of the dark pion is 5 GeV, the signal acceptance using this approach do not exceed 40% at large masses of the mediators. (see Fig. 4 of [11]).

Dark pion decay length defines the distance from the interaction point where a jet emerges. The emerging jet contains multiple displaced vertices, which con be reconstructed using a tracker [11]. Such jets can also be reconstructed using calorimeters with the timing layers. This method is expected to have advantage when the dark pion decay length is significant and the tracker cannot be efficient in reconstructing such tracks. It was also pointed out [10] that the emerging jets may have significant fraction of neutral particles and the reconstruction using charged tracks can have a low acceptance.

To estimate the performance of the timing layers in reconstructing emerging jets, we will use the same Monte Carlo settings as for Ref. **??**: The $pp$ collision event samples are generated with the "hidden valley" model framework in PYTHIA 8.2 assuming the centre-of-mass energy of 13 TeV, a fixed mass of 5 GeV for the dark pions. The samples were created after changing the decay distance $c\tau$ of the dark pions. The mass $Mx$ of the mediator was also varied.

To calculate the acceptance, will use the formalism based on Eq. 1, where $L = c\tau$, and $m$ is the mass of the dark pion, i.e. $L$ can be considered as a travel distance. After the dark pion creates a Standard Model jet, we assume that such jets travel to the surface of the timing layer with the same speed for all values of $m$. For the timing layers, the signature of emerging jets is time delays compared to the other (Standard Model) jets. The production vertex cannot be observed by the timing layers

if such jets emerges before TL1[1] After events being generated, the weighted average of the decay distances of all particles that originate from the dark pions, using the particle momentum as the weight, was calculated. This decay distance is used to approximate the decay length, without using a jet reconstruction. The calculation for the $3\sigma$ separation assumed $m_F = m_\alpha \simeq 3.73$ GeV although such a choice can be rather arbitrary. This value of $m_F$ is used to give a conservative estimate of the arrival time of the Standard Model jets. (One can argue that the Standard Model jets mainly consist of light-flavour hadrons and photons, therefore, $m_F$ is significantly lower).

The acceptance of reconstruction of the emerging jets events was calculated by counting the number of events that pass the Eq. 1 condition with the parameters as discussed before, divided by the total number of entries without this requirement. Figure 5 shows the acceptance as a function of the mediator mass $Mx$ and the decay distance of the dark pions. This figure can directly be compared to the similar acceptance figure for the method based on tracks [11]. The acceptance based on the TOF is significantly larger for low $Mx$ and large $c\tau$ of the pions, compared to a similar acceptance distribution based on tracking information. The acceptance is larger for the timing layers smaller than 100 ns, than for the standard 1 ns calorimeter resolution.

Now we will be interested in the acceptance of the reconstruction of dark pions as a function of their mass and the lifetime, but assuming a fixed mass $Mx$ for the mediator. This time we will consider the HE-LHC environment with $pp$ collisions at the centre-of-mass energy of 27 TeV. The Monte Carlo settings for the signal model were similar to those discussed in [11], but then were further tuned [12] to obtain samples which were most suitable for the detector performance studies. The mass of the mediator was set to 10 TeV, while the mass of the dark pion was varied in the range between 5 and 1000 GeV. The dark pion proper decay length, $c\tau$, was varied between 1 and 1000 mm (independent of its mass). Other parameters were also appropriately modified to allow a sufficient phase space for the dark meson production. The mass of the dark pion is assumed to be one half the mass of the dark quark. The mass of the dark $\rho$ is four times of the dark pion mass. The width of the mediator particle is assumed to be small as compared with the detector mass resolution.

As before, the acceptance of reconstruction of the emerging jets by measuring the timing information was calculated by counting the number of events that pass the Eq. 1 conditions with the parameters as discussed before, divided by the total number of entries without this requirement. Figure 6 shows the efficiency as a function of the $c\tau$ and the mass of the dark pion. It can be seen that a detector with the standard 1 ns resolution does not have acceptance for the dark meson measurements. The acceptance is significantly larger for the timing layers smaller than 100 ns. The acceptance is small for low $c\tau$ or small masses, which is the expected feature of the timing measurement. The timing layers with 20 ps have have 100% acceptance for large values of $c\tau$ and dark-meson masses. The efficiency as a function of the particle velocity for 20 ps and 1 ns timing layer resolutions is shown in the Appendix Appendix A.

Note that these results are relatively general since they are independent of the position of the timing layers, and other details relevant to the geometry of the calorimeter.

[1] It is possible that if such jets is created in the area between TL1 and TL2, such signatures can also be detected, but we will not consider this case.

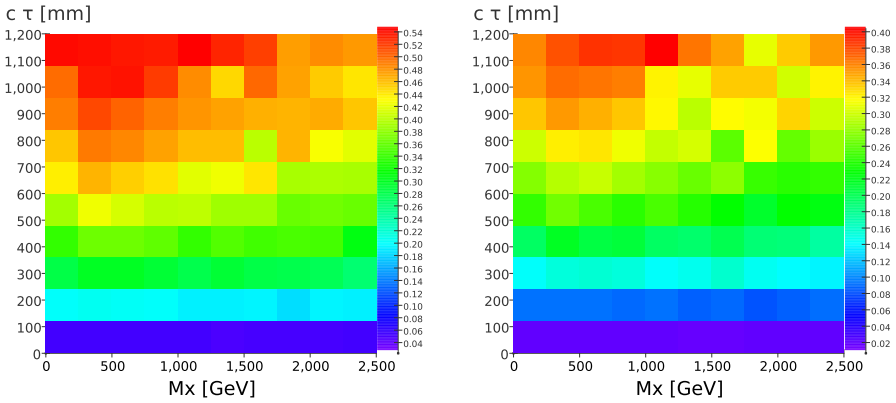


(a) 10 ps




(b) 20 ps

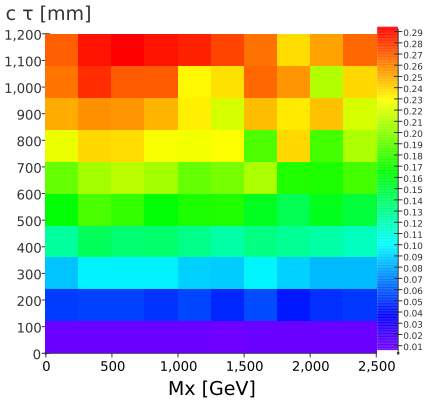


(c) 30 ps

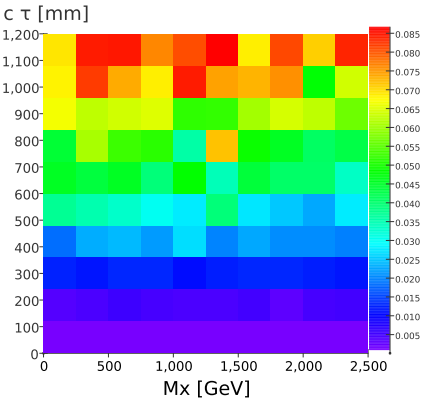


(d) 100 ps

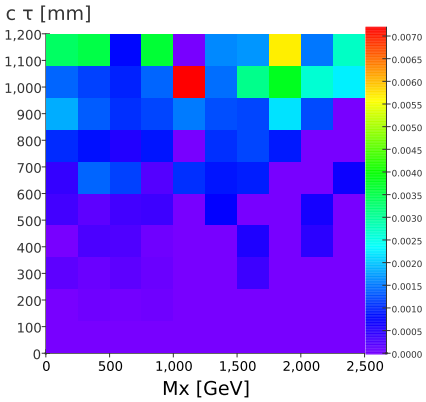


(e) 500 ps

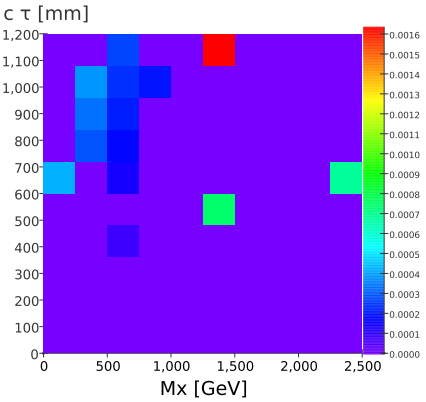


(f) 1000 ps

Figure 5: The acceptance for the reconstruction of emerging jets using the timing layers with different timing resolutions as a function of the mediator mass $Mx$ and the $c\tau$ of the dark pions with the mass 5 GeV. The Pythia8 simulations are performed for the $pp$ collisions at $\sqrt{s} = 13$ TeV.

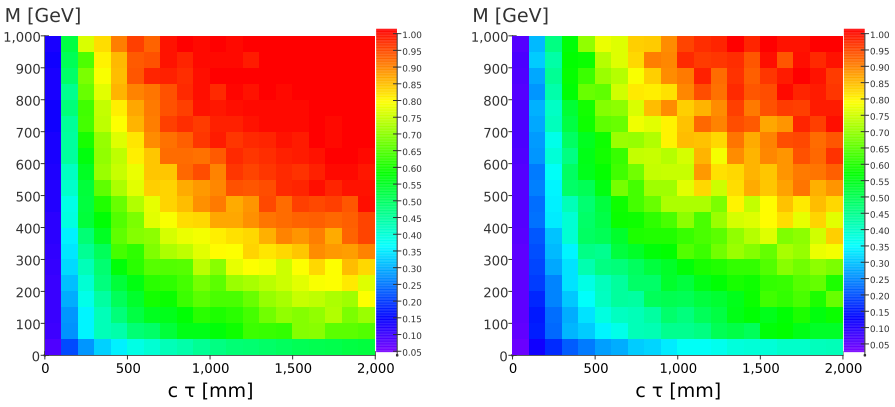


(a) 10 ps




(b) 20 ps

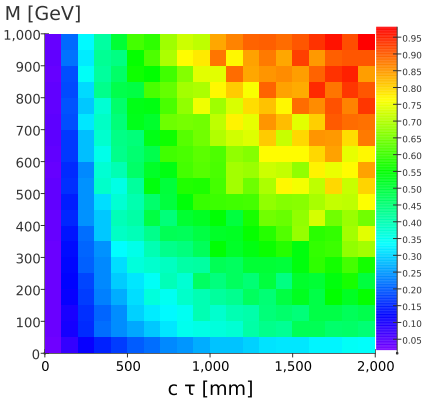


(c) 30 ps

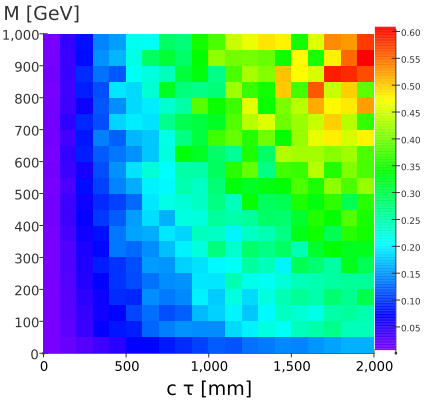


(d) 100 ps

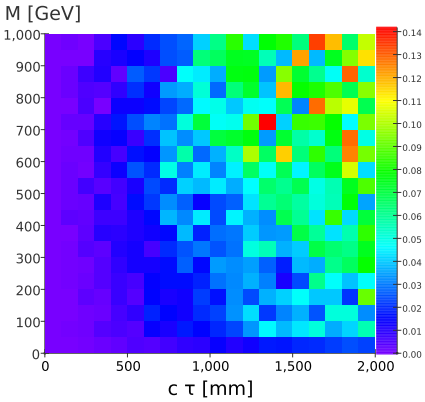


(e) 500 ps

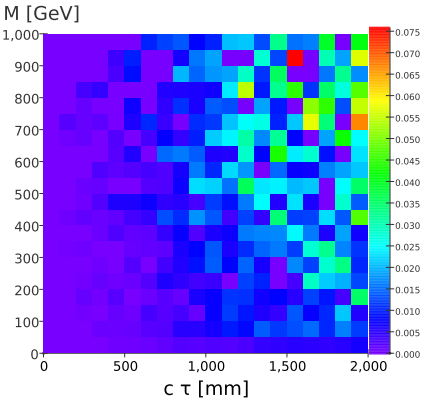


(f) 1000 ps

Figure 6: The acceptance for the reconstruction of emerging jets using the timing layers with different timing resolutions as as function of the mass of the dark pions and their $c\tau$. The mediator mass was fixed to 10 TeV. The Pythia8 simulations are performed for the $pp$ collisions at $\sqrt{s} = 27$ TeV.

## 5. Summary

This paper discusses the benefits of the timing layers positioned in front of the hadronic calorimeters. We have illustrated how such layers can be used for single particle identification, jets measurements, and identification of heavy long-lived particles in the context of the dark QCD model.

[1] L. Linssen, A. Miyamoto, M. Stanitzki, H. Weerts, Physics and Detectors at CLIC: CLIC Conceptual Design Report, CERN Yellow Reports: Monographs, CERN, Geneva, 2012, comments: 257 p, published as CERN Yellow Report CERN-2012-003. doi:10.5170/CERN-2012-003.
URL http://cds.cern.ch/record/1425915

[2] T. Behnke, J. E. Brau, B. Foster, J. Fuster, M. Harrison, J. M. Paterson, M. Peskin, M. Stanitzki, N. Walker, H. Yamamoto, The International Linear Collider Technical Design Report - Volume 1: Executive SummaryarXiv:1306.6327.

[3] M. Benedikt, The Global Future Circular Colliders EffortCERN-ACC-SLIDES-2016-0016. Presented at P5 Workshop on the Future of High Energy Physics, BNL, USA, Dec. 15-18, 2013.
URL http://cds.cern.ch/record/2206376

[4] J. Tang, et al., Concept for a Future Super Proton-Proton Collider (2015). arXiv:1507.03224.

[5] Z. Ahmed, et al., New Technologies for Discovery, in: CPAD Instrumentation Frontier Workshop 2018: New Technologies for Discovery IV (CPAD 2018) Providence, RI, United States, December 9-11, 2018, 2019. arXiv:1908.00194.
URL https://lss.fnal.gov/archive/2019/conf/fermilab-conf-19-487-di-nd-ppd-scd.pdf

[6] J. Allison, et al., Recent developments in Geant4, Nuclear Instruments and Methods in Physics Research A 835 (2016) 186.

[7] S. V. Chekanov, M. Beydler, A. V. Kotwal, L. Gray, S. Sen, N. V. Tran, S. S. Yu, J. Zuzelski, Initial performance studies of a general-purpose detector for multi-TeV physics at a 100 TeV pp collider, JINST 12 (06) (2017) P06009. arXiv:1612.07291, doi:10.1088/1748-0221/12/06/P06009.

[8] O. Cerri, S. Xie, C. Pena, M. Spiropulu, Identification of Long-lived Charged Particles using Time-Of-Flight Systems at the Upgraded LHC detectors, JHEP 04 (2019) 037. arXiv:1807.05453, doi:10.1007/JHEP04(2019)037.

[9] Y. Bai, P. Schwaller, Scale of dark QCD, Phys. Rev. D89 (6) (2014) 063522. arXiv:1306.4676, doi:10.1103/PhysRevD.89.063522.

[10] P. Schwaller, D. Stolarski, A. Weiler, Emerging Jets, JHEP 05 (2015) 059. arXiv:1502.05409, doi:10.1007/JHEP05(2015)059.

[11] CMS Collaboration, A. M. Sirunyan, et al., Search for new particles decaying to a jet and an emerging jet, JHEP 02 (2019) 179. arXiv:1810.10069, doi:10.1007/JHEP02(2019)179.

[12] K. Pedro, P. Schwaller, Private communication. We thank Dr. P.Kevin and P.Schwaller for help with the setup of Monte Carlo generation parameters.

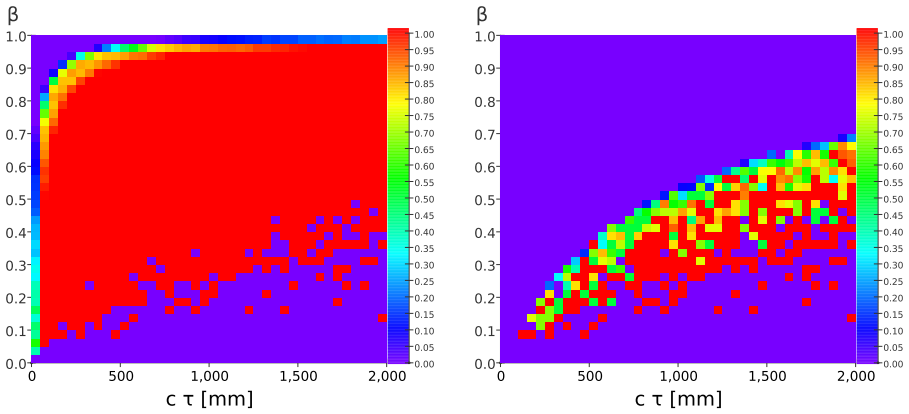


(a) 20 ps (b) 1000 ps

Figure A.7: The efficiency for the reconstruction of emerging jets using the timing layers with different timing resolutions. The plot shows the efficiency as a function of $c\tau$ and the particle velocity $\beta$

# Appendices

## Appendix A. Appendix

Figure A.7 shows the reconstruction efficiency as a function of $c\tau$ and the particle velocity $\beta = |p|/E$, for the two extreme cases of the timing layers.